

Conditional DETR V2: Efficient Detection Transformer with Box Queries

Xiaokang Chen¹, Fangyun Wei², Gang Zeng¹, and Jingdong Wang³

¹ Key Laboratory of Perception (MoE), School of AI, Peking University
² Microsoft Research Asia ³ Baidu

Abstract. In this paper, we are interested in Detection Transformer (DETR), an end-to-end object detection approach based on a transformer encoder-decoder architecture without hand-crafted postprocessing, such as NMS. Inspired by Conditional DETR, an improved DETR with fast training convergence, that presented box queries (originally called spatial queries) for internal decoder layers, we reformulate the object query into the format of the box query that is a composition of the embeddings of the reference point and the transformation of the box with respect to the reference point. This reformulation indicates the connection between the object query in DETR and the anchor box that is widely studied in Faster R-CNN. Furthermore, we learn the box queries from the image content, further improving the detection quality of Conditional DETR still with fast training convergence. In addition, we adopt the idea of axial self-attention to save the memory cost and accelerate the encoder. The resulting detector, called Conditional DETR V2, achieves better results than Conditional DETR, saves the memory cost and runs more efficiently. For example, for the DC5-ResNet-50 backbone, our approach achieves 44.8 AP with 16.4 FPS on the COCO *val* set and compared to Conditional DETR, it runs 1.6× faster, saves 74% of the overall memory cost, and improves 1.0 AP score.

1 Introduction

Object detection is a problem of localizing the objects and predicting their categories. It is a fundamental and challenging problem in computer vision [5,35,36,8,7,6] and has many practical applications, such as robot navigation and autonomous driving. Deep learning has been the dominant solution to object detection. The early framework regresses the object box by starting from a default box (or anchor box) and optionally iteratively refines the box regression, e.g., Faster R-CNN [30]. Recently, detection transformer (DETR) exploits the transformer decoder for object detection, with introducing the object queries (learnable positional embeddings). It is an end-to-end solution without the post-processing, such as non-maximum suppression (NMS).

DETR typically needs 500 epochs to achieve satisfactory performance. Several follow-up works, [34,13,42,25,11,48] develop DETR variants to accelerate the training process. Conditional DETR [25] and Anchor DETR [42] identify that

the decoder cross-attention has limited capability to exploit the spatial attention and designs the new query format to boost the capability.

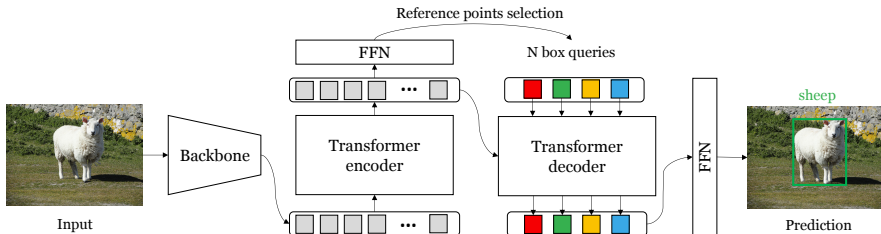


Fig. 1. The overall architecture. (1) We use a conventional CNN backbone (*e.g.*, ResNet-50) to extract the feature of an input image. (2) The learned embedding is fed into the transformer encoder layers to model the global dependencies between the inputs. (3) Then, we predict candidate boxes from the encoder embedding and select reference points according to the classification score of these boxes. The input of the decoder is the concatenation of the box query and the content query. The box query consists of the embedding of the selected reference points and the transformation predicted from the corresponding encoder embedding of these reference points. The content query is initialized from the selected candidate boxes. (4) We pass each output embedding of the decoder to a shared feed-forward network (FFN) that predicts either a detection (class and bounding box) or a “no object” class.

Inspired by the spatial queries (we call box queries) that Conditional DETR introduces for internal decoder layers, we propose to study the object query (positional encodings), the input of the first decoder layer, and reformulate it as the form of the box query in the embedding space. The box query is a composition of the embeddings of the reference point and the transformation of the box with respect to the reference point. The box query form in some sense builds the connection between DETR and Faster R-CNN that both use the boxes as one input. There are several differences. The box query is in the embedding space and the anchor box is in a form of 2D coordinates. The box query is explored through the attention mechanism to find the extremities for box regression and the regions inside the object for classification, while the anchor box is used as the initial guess.

We predict the box queries from the image content for each image, instead of learning them as model parameters.

Specifically, we predict the probability of belonging to an object for the points in the encoder embedding, and select the top-scored points as the reference points. The transformation that contains the scale information of the object is predicted from the corresponding encoder embedding. The image-dependent box query helps locate the object and improve the performance.

In addition, we adopt the idea of axial self-attention [16] and propose the Horizontal-Vertical Attention. For each query embedding, we perform attention

in the horizontal and vertical directions in parallel. Experiments show that the Horizontal-Vertical Attention could save the memory cost and accelerate the encoder, especially for high-resolution backbones, such as DC5-ResNet-50 and DC5-ResNet-101.

2 Related Work

Anchor-based object detectors. Anchor plays an important role in object detection. Faster R-CNN [30] first introduces the anchor boxes to make dense predictions. A series of works such as SSD [22], RetinaNet [20], YOLO [28,29,2] and Cascade R-CNN [3] are proposed to make object detection more efficient and accurate. To avoid hand-crafted anchor design, some recent methods, e.g. FCOS [37], CenterNet [46], CornerNet [19] and ExtremeNet [47], use anchor points to represent objects, these methods are also known as anchor-free detectors.

In this paper, we reformulate the object query in DETR into the format of the box query that consists of the embeddings of the reference point and the transformation of the box with respect to the reference point. This reformulation indicates the connection between the object query in DETR and the anchor box in Faster R-CNN.

DETR and its variants. DETR successfully applies transformers to object detection and removes the need for non-maximum suppression. The object queries (or called position embeddings) in DETR are responsible for the category prediction and box regression of each object. Some works [48,41] aim to solve the high computation complexity issue caused by the global encoder self-attention in DETR. Deformable DETR [48] designs the sparse attention that each query only attends to keys in a local region. PNP-DETR [41] proposes the poll-and-pool strategy to reduce the spatial redundancy in the input, resulting in a smaller input size for the encoder.

DETR also suffers from another issue, the slow training convergence, which attracts a lot of attention. TSP [34] eliminates the cross-attention modules and combines the FCOS and R-CNN-like detection heads. Deformable DETR [48] proposes deformable attention and uses multiple level features to accelerate the converge. SMCA[13] modulates the DETR multi-head global cross-attentions with gaussian maps around a few (shifted) centers to focus more on the restricted local regions.

Anchor DETR [42] argues that object query in DETR could not focus on a specific region and replace object queries with anchor points. Conditional DETR [25] proposes to search the extremity and distinct regions of the object through learning the conditional spatial queries from the decoder embeddings. However, the spatial query of the first layer could not find such regions well due to the lack of the image content in the query. To solve this issue, we propose the box query and initialize it from the image content, which could find extremity regions since the first layer.

Efficient attention mechanism. The global self-attention [39] could model the global dependencies between the inputs, while the computation complexity is quadratic to the input size. Many efficient attention mechanisms have been designed in the NLP field to improve the memory and computation efficiency of self-attention, such as Sparse Transformer [9], Linformer [40], Performer [10], RFA [26], Nystromformer [43], Reformer [18], Routing Transformer [33], Big-Bird [45], Longformer [1], Transformer-XL [12]. In the vision field, some methods [27,38] restrict the attention region of the key for each query instead of the whole region. For example, Swin Transformer [23] and HRFormer [44] adopt the local self-attention mechanism and add interaction across different local windows. Axial self-attention [16] applies the local window along the horizontal or vertical axis sequentially to achieve global attention. Following axial self-attention, we propose the Horizontal-Vertical Attention, where each query pixel attends to pixels that belong to the same row or column as it in parallel.

3 Approach

3.1 Architecture

We follow detection transformer (DETR) to use the transformer encoder and decoder structure for object detection. The architecture consists of a CNN backbone, a transformer encoder, a transformer decoder, and predictors for classification and box regression. The transformer encoder aims to improve the content embeddings output from the CNN backbone. It is a stack of multiple encoder layers, where each layer mainly consists of a self-attention layer and a feed-forward layer.

The transformer decoder is a stack of decoder layers. Each decoder layer is composed of three main layers: (1) a self-attention layer with the embeddings, outputted from the previous decoder layer as the input, (2) a cross-attention layer, with the output of the self-attention layer as the queries and the output of the encoder forming the keys and the values, and (3) a feed-forward layer predicting the box and the category score.

A candidate box is predicted from each decoder embedding as follows,

$$\hat{\mathbf{b}} = \text{sigmoid}(\text{FFN}(\mathbf{f}) + [\mathbf{s}^\top \ 0 \ 0]^\top). \quad (1)$$

Here, \mathbf{f} is the decoder embedding. $\hat{\mathbf{b}}$ is a four-dimensional vector $[b_{cx} \ b_{cy} \ b_w \ b_h]^\top$, consisting of the box center, the box width and the box height. \mathbf{s} is the unnormalized 2D coordinate of the reference point, and is $(0, 0)$ in the original DETR. The classification score for each candidate box is also predicted from the decoder embedding through another FNN, $\mathbf{e} = \text{FFN}(\mathbf{f})$.

3.2 Box Query

Object query. The original DETR learns *object queries*,

$$\{\mathbf{o}_1, \dots, \mathbf{o}_N\}, \quad (2)$$

where each query is a high-dimensional embedding vector. These object queries are model parameters and are the same for all the images. In DETR [4], they are also called positional encodings, and initially used to encode the information of the positions at which the objects might appear. The object queries are combined into the decoder embeddings, forming the queries of the self-attention and cross-attention layers in the decoder.

Box query. Conditional DETR learns spatial queries, which we call box queries in this paper, from the decoder output embeddings and use them to replace the object queries for the decoders except for the first decoder layer. The box queries are combined with the content queries through concatenation instead of addition in the original DETR. Accordingly, the keys are formed by concatenating the positional embeddings and the encoder output embeddings.

The box queries \mathbf{p}_q are predicted by transforming the 2D reference point in the embedding space with the transformation of the box with respect to the reference point:

$$\mathbf{p}_q = \lambda_q \odot \mathbf{p}_s. \quad (3)$$

Here, \mathbf{p}_s is the projected positional embedding from the reference point and λ_q is a transformation in the embedding space. \odot is the element-wise multiplication operator.

Learning initial box queries as model parameters. We use the box queries to replace the object queries that Conditional DETR still uses in the first decoder layer. We learn 2D reference points, $\{(c_{x1}, c_{y1}), \dots, (c_{xK}, c_{yK})\}$, and use the sinusoidal positional embedding to form the corresponding embeddings $\{\mathbf{p}_{s1}, \dots, \mathbf{p}_{sK}\}$. λ_q is set as the model parameter that is randomly initialized.

Predicting initial box queries from image content. The pipeline is shown in Figure 2. We propose to select several positions as reference points, $\{(c_{x1}, c_{y1}), \dots, (c_{xK}, c_{yK})\}$ from the image content. We then build the reference embeddings from these points and the transformation for each reference point according to the corresponding encoder embedding $\hat{\mathbf{X}}$ as the following,

$$\lambda_q = \text{FFN}(\hat{\mathbf{x}}(c_x, c_y)), \quad (4)$$

where $\hat{\mathbf{x}}(c_x, c_y)$ is the encoder embedding at the position (c_x, c_y) . (c_x, c_y) is the normalized position which ranges from 0 to 1. We select the reference positions by classifying each position. The classification score is also predicted from the encoder embedding through an FFN,

$$\mathbf{s} = \text{FFN}(\hat{\mathbf{x}}(c_x, c_y)). \quad (5)$$

We perform binary classification here and \mathbf{s} is a 2-d vector, indicating the possibility of being an object (1) or non-object (0). We rank all the positions according to their probability of being an object and the top-scored predictions are selected.

The purpose of using image content is different from the two-stage strategy in Deformable DETR. They generate the initial positions and box sizes from

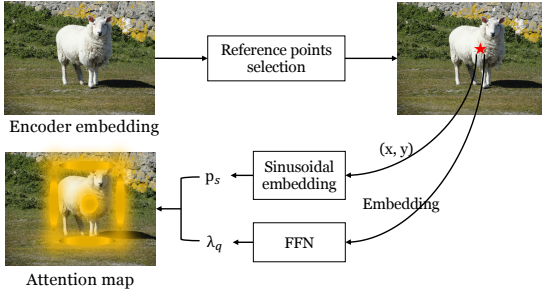


Fig. 2. Pipeline of box query initialization. The box query is a composition of the embeddings of the box center (reference point) and the box size. The attention map is a toy example, not the actual output from the model.

the image content, then sample the key set around those positions. The final box size is predicted based on the initial box size, which is a form of residual prediction and easier to optimize. By contrast, we project the position and box information to high-dimensional space and use them to form the box query. The box query could scale the range that we search for the object according to its size.

Initial content queries from image. In the internal decoder layers, the content query, output from the previous decoder layer, is used to predict the box, indicating that the content query also contains the box information. In light of this, we initialize the content query for the first decoder layer by incorporating the box information.

We consider two ways. One is to initialize the content query from the encoder embeddings:

$$\mathbf{c}_q = \text{FFN}(\hat{\mathbf{x}}(c_x, c_y)). \quad (6)$$

The other one uses the box estimated from the position:

$$\mathbf{c}_q = \text{FFN}(\text{PE}(\mathbf{b}(c_x, c_y))). \quad (7)$$

Here, $\mathbf{b}(c_x, c_y)$ is the box estimated from the position (c_x, c_y) : $\text{sigmoid}(\text{FFN}(\hat{\mathbf{x}}(c_x, c_y)) + \sigma^{-1}([c_x \ c_y \ c_w \ c_h]^\top))$, and $\text{PE}()$ is the positional embedding. σ^{-1} means the inverse sigmoid function. c_w and c_h are hyper-parameters and we will study them in the experiment section. Our results empirically indicate that the two ways perform similarly and the latter way performs slightly better.

3.3 Horizontal-Vertical Attention

The encoder attention is formulated as follows,

$$\text{Atten}(\mathbf{x}_{uv}, \mathbf{X}, \mathbf{X}) = \sum_{i=1}^H \sum_{j=1}^W \mathbf{x}_{ij} \alpha(\mathbf{x}_{uv}, \mathbf{x}_{ij}). \quad (8)$$

$$\alpha(\mathbf{x}_{uv}, \mathbf{x}_{ij}) = \frac{e^{\frac{1}{\sqrt{d}} \mathbf{x}_{uv}^{\top} \mathbf{x}_{ij}}}{\sum_{i=1}^H \sum_{j=1}^W e^{\frac{1}{\sqrt{d}} \mathbf{x}_{uv}^{\top} \mathbf{x}_{ij}}}. \quad (9)$$

Here \mathbf{X} is the embedding output from the backbone, *e.g.*, ResNet-50. We use one query \mathbf{x}_{uv} at the position (u, v) as an example. d is the feature dimension. The memory and computation complexities for all the HW queries are quadratic with respect to the map size HW .

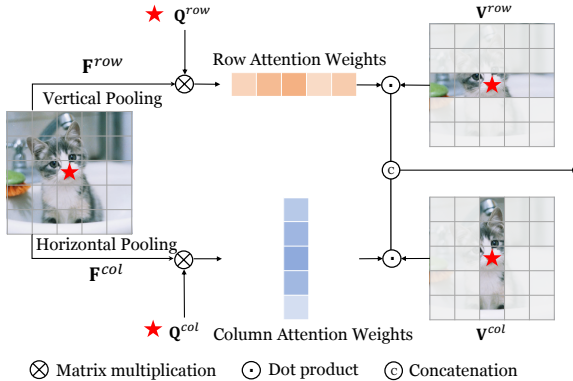


Fig. 3. The proposed Horizontal-Vertical Attention. Each pixel will aggregate embeddings of the pixels in the same row or column. \mathbf{Q}^{row} (\mathbf{Q}^{col}) is generated by the addition of the query embedding and the 1D row (col) position encoding. \mathbf{F}^{row} (\mathbf{F}^{col}) is generated by the addition of the pooled row (col) embedding and the 1D row (col) position encoding. \mathbf{V}^{row} (\mathbf{V}^{col}) is from the pixels that lie in the same row (col) as the query pixel.

We propose to decrease the number of keys for complexity reduction, as shown in Figure 3. The idea is inspired by CCNet [17] and axial self-attention [16]. We pool the embedding \mathbf{X} along the vertical and horizontal directions respectively, $\bar{\mathbf{x}}_{:j} = \frac{1}{H} \sum_{i=1}^H \mathbf{x}_{ij}$, and $\bar{\mathbf{x}}_i = \frac{1}{W} \sum_{j=1}^W \mathbf{x}_{ij}$, and form $(H + W)$ keys:

$$\mathbf{K} = [\bar{\mathbf{x}}_1: \dots \bar{\mathbf{x}}_H: \bar{\mathbf{x}}_{:1} \dots \bar{\mathbf{x}}_{:W}]. \quad (10)$$

The HV-attention process is as follows,

$$\text{HV-Atten}(\mathbf{x}_{uv}, \mathbf{K}, \mathbf{X}) = \text{Concat}\left(\sum_{i=1}^H \mathbf{x}_{iv} \alpha(\mathbf{x}_{uv}, \bar{\mathbf{x}}_{i:}), \sum_{j=1}^W \mathbf{x}_{uj} \alpha(\mathbf{x}_{uv}, \bar{\mathbf{x}}_{:j})\right). \quad (11)$$

Complexity analysis. The computation complexity of HV-attention is reduced from quadratic to linear with respect to HW . The computational complexity of global self-attention and our Horizontal-Vertical Attention based on the feature map $\mathbf{F} \in \mathbb{R}^{d \times H \times W}$ are:

$$\Omega(\text{Global-Atten}) = 4HWd^2 + 2(HW)^2d, \quad (12)$$

$$\Omega(\text{HV-Atten}) = 7HWd^2 + 2HWd(H + W), \quad (13)$$

where the coefficient of the first item increases from 4 to 7 because we apply two linear projections on the query, key and value. Eq. (12) is quadratic to HW and is unaffordable when HW is large.

Comparison with CC Attention [17]. The process of CC Attention is as follows,

$$\mathbf{K}_{uv} = [\mathbf{x}_{1v}, \dots, \mathbf{x}_{Hv}, \mathbf{x}_{u1}, \dots, \mathbf{x}_{uW}]. \quad (14)$$

$$\text{CC-Atten}(\mathbf{x}_{uv}, \mathbf{K}_{uv}, \mathbf{X}) = \sum_{i=1}^H \mathbf{x}_{iv} \alpha(\mathbf{x}_{uv}, \mathbf{x}_{iv}) + \sum_{j=1}^W \mathbf{x}_{uj} \alpha(\mathbf{x}_{uv}, \mathbf{x}_{uj}). \quad (15)$$

Here \mathbf{X} is the embedding output from the backbone, *e.g.*, ResNet-50. We use one query \mathbf{x}_{uv} at the position (u, v) as an example. \mathbf{K}_{uv} is the key set for the query position (u, v) . There are two differences between our method and CC Attention. (1) We use a shared key set for all the queries, further saving the memory cost of the attention module. For example, 13% memory cost is saved for the $256 \times 100 \times 150$ ($d \times H \times W$) input. (2) We use concatenation instead of addition when aggregating the horizontal and vertical features, which brings 0.5 AP improvement ($44.3 \rightarrow 44.8$) on the DC5-ResNet-50 backbone.

Comparison with RCDA [42]. We also compare our Horizontal-Vertical Attention with the Row-Column Decoupled Attention (RCDA). RCDA decouples the 2D key feature to the row feature and the column feature by 1D global average pooling, and performs the row attention and the column attention successively. Our proposed method is different from them in that: (1) We conduct row attention and column attention in a parallel way. (2) The value set we use is the feature of pixels that belong to the same row or column as the query pixel,



Fig. 4. Illustrating the spatial attention weight maps from **the first decoder layer**. For each scene, the upper row is from the model with random initialized box query and the lower row is from the model with image-dependent box query. The attention weight maps are from 5 heads out of the 8 heads and the green box in each image is the ground-truth box. Best viewed in color.

while RCDA views all the pixels as the value set, bringing more computational cost.

3.4 Visualization

Figure 4 visualizes the spatial attention weight maps of the first decoder layer. The upper row of each scene adopts the randomly initialized box query, and the lower row is our image-dependent box query. The maps are soft-max normalized over the dot products between the box query and the position embedding of the key. We show 5 out of the 8 maps, and the other three are duplicates. The duplicates might be different for models trained several times, but the detection performance is almost the same.

In the visualizations of our method, the spatial attention map in the first four columns highlights an extremity region near a certain edge of the bounding box, *e.g.*, the head of the cat in the second row. The map in the last column highlights a small region inside the box, whose representations might already encode enough information for object classification. We also find that the image-dependent box

query is able to scale the spatial spread for the extremity it highlights. For a larger object, such as the bus in the last row, our method highlights a larger spread. For a smaller object, such as the cat in the second row, our method highlights a smaller spread.

By contrast, the spatial attention map of the randomly initialized box query does not show this property. Each head only highlights a small region near the object center. Although a certain head may try to find an extremity region, such as the fourth column, it could not scale the spatial spread of the highlight regions according to the object size.

3.5 Discussion: Box Query vs Anchor Box

The box query builds the connection between DETR and Faster R-CNN. They both use the form of boxes as one input and extract features according to the box. However, there are some differences. (1) The box query is in the embedding space, which consists of the embedding of the reference point and the transformation. The transformation could transform the embedding of the reference point to the extremity regions of the object, which is like a box. The anchor box is in the form of 2D coordinates, consisting of box center and box height/width. (2) The box query is explored through the attention mechanism to find the extremities of the object for box regression and the regions inside the object for classification. While the anchor box is used as the initial guess and all areas in the box are treated as the region of interest (ROI), which is used for classification and box regression.

3.6 Loss Function

The box query and the content query are initialized from the top-scored candidate boxes. We supervise the box predictions and view it as a bipartite matching problem between the predicted boxes and the ground-truth boxes.

The matching cost is defined as:

$$\mathcal{C}_{\text{match}} = \sum_{i=1}^G [\mu_{\text{cls}} \ell_{\text{FL}}(\mathbf{p}_{\xi(i)}, \bar{c}_i) + \ell_{\text{box}}(\mathbf{b}_{\xi(i)}, \bar{\mathbf{b}}_i)]. \quad (16)$$

Here G is the number of ground-truth objects. ℓ_{FL} is the focal loss and $\mu_{\text{cls}} = 2$ is the trade-off coefficient. \bar{c}_i is the class of the i th ground-truth box and $\bar{c}_i = \text{null}$ if $i > G$. We binarize the ground-truth label and $\bar{c}_i = 1$ if it is an object. $\bar{\mathbf{b}}_i$ is the i th ground-truth box and ℓ_{box} is a combination of ℓ_1 loss and GIoU loss [32] and the loss weights are 5 and 2, respectively.

$\xi(\cdot)$ is a permutation of N predictions and we could find an optimal solution $\hat{\xi}(\cdot)$ through minimizing the matching cost. Then the loss function to supervise the initialization of the box query and the content query is computed as:

$$\mathcal{L}_{\text{init}} = \sum_{i=1}^N \lambda_{\text{cls}} \ell_{\text{FL}}(\mathbf{p}_{\hat{\xi}(i)}, \bar{c}_i) + \delta_{[i \leq G]} \ell_{\text{box}}(\mathbf{b}_{\hat{\xi}(i)}, \bar{\mathbf{b}}_i), \quad (17)$$

where $\lambda_{\text{cls}} = 2$ is the trade-off coefficient. δ is the indicator function. We use the same loss function as Conditional DETR [25] to supervise the output of the decoder, which is noted as \mathcal{L}_{dec} . Then the overall loss function is defined as:

$$\mathcal{L} = \mathcal{L}_{\text{init}} + \mathcal{L}_{\text{dec}}. \quad (18)$$

4 Experiments

4.1 Setting

Dataset. We perform the experiments on the COCO 2017 [21] detection dataset, which contains about 118K training (**train**) images and 5K validation (**val**) images.

Table 1. Comparison of Conditional DETR V2 with other detection models on COCO 2017 **val**. * means these methods use multi-scale feature. + means we use 900 box queries.

Model	#epochs	GFLOPs	#params	AP	AP ₅₀	AP ₇₅	AP _S	AP _M	AP _L
DETR-R50 [4]	500	86	41M	42.0	62.4	44.2	20.5	45.8	61.1
DETR-R50 [4]	50	86	41M	34.9	55.5	36.0	14.4	37.2	54.5
PNP-DETR-R50 [41]	500	82	41M	41.8	62.1	44.4	21.2	45.3	60.8
Deformable DETR-R50 [48]	50	78	34M	39.4	59.6	42.3	20.6	42.9	55.5
UP-DETR-R50 [11]	150	86	41M	40.5	60.8	42.6	19.0	44.4	60.0
Anchor DETR-R50 [42]	50	94	37M	42.1	63.1	44.9	22.3	46.2	60.0
Conditional DETR-R50 [25]	50	90	44M	40.9	61.8	43.3	20.8	44.6	59.2
Conditional DETR V2-R50	50	89	46M	42.5	63.4	44.9	22.5	45.9	61.4
DETR-DC5-R50 [4]	500	187	41M	43.3	63.1	45.9	22.5	47.3	61.1
DETR-DC5-R50 [4]	50	187	41M	36.7	57.6	38.2	15.4	39.8	56.3
Faster RCNN-FPN-R50* [31]	108	180	42M	42.0	62.1	45.5	26.6	45.5	53.4
TSP-RCNN-R50* [34]	36	188	–	43.8	63.3	48.3	28.6	46.9	55.7
SMCA-R50* [13]	50	152	40M	43.7	63.6	47.2	24.2	47.0	60.4
PNP-DETR-DC5-R50 [41]	500	144	41M	43.1	63.4	45.3	22.7	46.5	61.1
Deformable DETR-DC5-R50 [48]	50	128	34M	41.5	61.8	44.9	24.1	45.3	56.0
Two-Stage Deformable DETR-DC5-R50 [48]	50	128	34M	43.6	63.6	47.0	25.8	46.6	58.1
Anchor DETR-DC5-R50 [42]	50	173	37M	44.2	64.7	47.5	24.7	48.2	60.6
Conditional DETR-DC5-R50[25]	50	195	44M	43.8	64.4	46.7	24.0	47.6	60.7
Conditional DETR V2-DC5-R50	50	161	46M	44.8	65.3	48.2	25.5	48.6	62.0
Conditional DETR V2-DC5-R50 ⁺	50	181	46M	45.2	66.0	48.4	26.5	49.0	62.1
DETR-R101 [4]	500	152	60M	43.5	63.8	46.4	21.9	48.0	61.8
DETR-R101 [4]	50	152	60M	36.9	57.8	38.6	15.5	40.6	55.6
Anchor DETR-R101 [42]	50	160	56M	43.5	64.3	46.6	23.2	47.7	61.4
Conditional DETR-R101 [25]	50	156	63M	42.8	63.7	46.0	21.7	46.6	60.9
Conditional DETR V2-R101	50	155	65M	43.9	65.3	46.7	25.2	48.0	62.6
DETR-DC5-R101 [4]	500	253	60M	44.9	64.7	47.7	23.7	49.5	62.3
DETR-DC5-R101 [4]	50	253	60M	38.6	59.7	40.7	17.2	42.2	57.4
Faster RCNN-FPN-R101* [31]	108	246	60M	44.0	63.9	47.8	27.2	48.1	56.0
TSP-RCNN-R101* [34]	36	254	–	44.8	63.8	49.2	29.0	47.9	57.1
SMCA-R101* [13]	50	218	58M	44.4	65.2	48.0	24.3	48.5	61.0
Anchor DETR-DC5-R101 [42]	50	239	56M	45.1	65.7	48.8	25.8	49.4	61.6
Conditional DETR-DC5-R101[25]	50	262	63M	45.0	65.5	48.4	26.1	48.9	62.8
Conditional DETR V2-DC5-R101	50	228	65M	45.5	66.0	48.7	26.3	49.0	62.9
Conditional DETR V2-DC5-R101 ⁺	50	247	65M	45.9	66.6	49.6	27.4	49.9	62.6
Conditional DETR-HR48 [25]	50	1090	87M	48.2	68.2	52.4	30.6	52.3	64.3
Conditional DETR V2-HR48	50	521	90M	49.8	70.2	54.2	32.1	53.3	65.9

Training. We follow the DETR training protocol [4]. The backbone is the ImageNet-pretrained model from TORCHVISION with batchnorm layers fixed, and the transformer parameters are initialized using the Xavier initialization scheme [14]. We train the model on the COCO training set for 50 epochs, with the AdamW [24] optimizer. The weight decay is set to be 10^{-4} . The learning rates for the backbone and the transformer are initialized as 10^{-5} and 10^{-4} , respectively. The learning rate is dropped by a factor of 10 after 40 epochs. The dropout rate in the transformer is 0.1. The head for the attention is 8, the attention feature channel is 256 and the hidden dimension of the feed-forward network is 2048. The number of box queries is set as 300 by default.

We use the augmentation scheme same as DETR [4]: resize the input image such that the short side is at least 480 and at most 800 pixels and the long side is at most 1333 pixels; randomly crop the image such that a training image is cropped with a probability 0.5 to a random rectangular patch.

Evaluation. We use the standard COCO evaluation. We report the average precision (AP), and the AP scores at 0.50, 0.75 and for the small, medium, and large objects.

4.2 Results

Table 1 shows comparison of the proposed method with other detection methods on COCO 2017 val. We first report the results of single scale methods: DETR [4], PNP-DETR [41], deformable DETR [48], UP-DETR [11], Anchor DETR [42] and Conditional DETR [25]. We follow [4] and report the results over four backbones: ResNet-50 [15], ResNet-101, and their $16\times$ -resolution extensions DC5-ResNet-50 and DC5-ResNet-101. The $16\times$ -resolution extensions are obtained by adding a dilation convolution in the last stage and removing a stride from the first convolution of the last stage. Our Conditional DETR V2 with 50 training epochs for R50 and R101 as the backbones not only outperforms Conditional DETR, but also outperforms DETR with 500 training epochs. When it comes to a higher-resolution backbone such as DC5-ResNet-50, our Conditional DETR V2 saves 17% GFLOPs and improves AP score by 1.0 compared to Conditional DETR.

In addition, we list some methods that use the multi-scale feature. Although our main purpose is not to study how to make better use of the multi-scale feature, our single-scale models still achieve similar performance to most of theirs. In the meanwhile, our computational cost (*e.g.*, GFLOPs) is lower than most of these methods and comparable to SMCA, which illustrates the effectiveness of the proposed method.

We also adopt HRNet-W48 as the backbone to verify the generalization ability of the proposed method. We down-sample the feature map from $4\times$ (the initial output of HRNet) to $8\times$ to save the computation cost. Results in Table 1 show that the proposed method outperforms Conditional DETR by 1.6 AP while saving 52% GFLOPs. This illustrates that the proposed method could generalize well to the high-resolution backbone.

4.3 Ablations

The effect of box query initialization. We empirically study how the model benefits from the image-dependent box query. We compare three ways to initialize the box query: (i) RB - we use the box queries to replace the object queries that Conditional DETR uses in the first decoder layer. The reference point and the transformation (λ_q) are randomly initialized. (ii) IP - the reference point is initialized from the image content and the λ_q is randomly initialized. This is similar to the two-stage strategy in Deformable DETR. (iii) IP+IT - both the reference point and the λ_q are initialized from the image content.

Table 2. The empirical results about the box query. RB = random box query. IP = image-dependent reference point. IT = image-dependent transformation. The backbone ResNet-50 is adopted. The Horizontal-Vertical Attention is not used here.

Method	GFLOPs	AP
Conditional DETR	89.5	40.9
Conditional DETR + RB	89.5	40.9
Conditional DETR + IP	90.0	41.9
Conditional DETR + IP + IT	90.1	42.9

Table 3. The empirical results about the choice of $[c_w c_h]$. The backbone ResNet-50 is adopted. The Horizontal-Vertical Attention is not used here.

$[0.1, 0.1]$	$[0.2, 0.2]$	$[0.4, 0.4]$	GFLOPs	AP
✓			89.8	42.2
	✓		89.8	42.2
		✓	89.8	42.3
✓	✓		90.0	42.6
✓	✓	✓	90.1	42.9

Table 4. The empirical results about the effect of $[c_x c_y]$ and $[c_w c_h]$ that used for content query initialization. The backbone ResNet-50 is adopted. The Horizontal-Vertical Attention is not used here.

$[c_x c_y]$	$[c_w c_h]$	GFLOPs	AP
✓		89.8	42.0
	✓	89.8	42.4
✓	✓	90.1	42.9

Results are reported in Table 2. We find the randomly initialized box query does not improve the performance, since the query has no image-dependent information. If we initialize the reference point with positions selected from the image content, the AP improves 1.0. This is reasonable because the initial reference points are likely in the object regions that we want to pay attention to. If

we further predict the transformation (λ_q) of the box query from the image content as well, which contains the scale information of the object, the performance improves to 42.9 AP. This indicates that both the initializations of the reference point and the transformation in the box query are important. With an appropriate transformation that contains scale information, we could dynamically adjust the spread of the attended regions for different objects.

The effect of content query initialization. We initialize the content query with the estimated box, as illustrated in Eq. (7). We first conduct experiments to verify how different choices of $[c_w, c_h]$ affect the performance. In implementation, we estimate three candidate boxes with different scales at each position and the $[c_w, c_h]$ are $[0.1, 0.1]$, $[0.2, 0.2]$ and $[0.4, 0.4]$, respectively. Please note that 0.1 is the normalized length, which is the ratio of box length to image length. In Table 3, we try different choices, *e.g.*, estimate one or two boxes at one position. Results show that with only one candidate box per position, the performance has already improved to 42.2 AP, which is 1.3 higher than Conditional DETR. When we estimate candidate boxes of two scales, the performance further improves. Three scales performs the best. This is because the model’s ability to detect objects of different scales is stronger.

When $[c_w, c_h]$ is set as $[0.1, 0.1]$, $[0.2, 0.2]$, $[0.4, 0.4]$, the AP scores for large objects are 61.3, 61.3, 62.0, and the AP scores for small objects are 22.3, 22.0, 21.9. With a larger initial scale, large objects will be easier to detect. The performance of small objects drops a little because it is harder to search for small objects with a too large initial scale.

Then, we verify the effect of $[c_x, c_y]$ and $[c_w, c_h]$ for content query initialization in Table 4. $[c_x, c_y]$ helps search the distinct region of the object for classification and $[c_w, c_h]$ helps search the region with similar scale for box regression. Using the two items together achieves the overall best result.

Table 5. The analysis of the computational cost and the speed. HVA = Horizontal-Vertical Attention. The backbone ResNet-50 and DC5-ResNet-50 are adopted. We follow DETR to test over the first 100 images of COCO 2017 val. The experiments are conducted on a single Tesla V100 GPU.

Method	Backbone	GFLOPs	Memory (M)	FPS	AP
Conditional DETR	ResNet-50	90	2887	22	40.9
Conditional DETR v2 w/o HVA	ResNet-50	90	2913	20	42.9
Conditional DETR v2	ResNet-50	89	2093	20	42.5
Conditional DETR	DC5-ResNet-50	195	18631	10	43.8
Conditional DETR v2 w/o HVA	DC5-ResNet-50	197	18748	10	44.8
Conditional DETR v2	DC5-ResNet-50	161	4844	16	44.8

Analysis of the computational cost and the speed. We compare the computational cost and speed of the proposed method to Conditional DETR in Table 5. For the ResNet-50 backbone, the proposed Horizontal-Vertical Attention reduces the memory cost significantly, but only 1G flops are saved. This is because the overall computational cost of the transformer head is relatively

Table 6. Inference speed and AP performance on COCO 2017 val. `TorchScript` is not used here. All models are trained with 50 epochs except DETR that is trained with 500 epochs. Our model achieves the best speed/accuracy trade-off.

Method	Inference Speed (FPS)	AP
DETR	10	43.3
SMCA	10	43.7
Conditional DETR	10	43.8
Anchor DETR	16	44.2
Conditional DETR v2	16	44.8

small for the $32\times$ feature. For the DC5-ResNet-50 backbone, the global self-attention consumes huge resources, *e.g.*, 18748 M memory. The speed is much slower due to the high computational complexity. With the help of the proposed Horizontal-Vertical Attention, the memory cost is reduced by 74% and the speed is increased by 60%. We also compare the efficiency to other DETR variants in Table 6, where we could find that our method achieves the best speed/accuracy trade-off.

5 Conclusion

We reformulate the object query in DETR to the format of the box query, which is a composition of the embedding of the reference point and the transformation of the box with respect to the reference point. We further learn the box query from the image content instead of setting them as the model parameters, which improves the detection performance. To save the memory cost of the transformer encoder, we learn from axial self-attention and propose to perform attention in horizontal and vertical directions in parallel. Experiments verify the efficiency of the proposed method.

A Visualization of the Reference Points

We select reference points from the image content, as illustrated in Section 3.2 in the main paper. We visualize the reference points in Figure 5 and find that the reference points mainly exist in the object regions. For example, in the last image of the second row, almost all the reference points are distributed on the three cows.



Fig. 5. Visualization of the reference points. We use 300 reference points in the model, which are marked with red in the images. Best viewed in color.

B Approach Details

Decoder cross attention weight. For the internal decoder layers, we calculate the decoder cross attention weight in the same way as Conditional DETR [25]:

$$\begin{aligned} & \mathbf{c}_q^\top \mathbf{c}_k + \mathbf{p}_q^\top \mathbf{p}_k \\ &= \mathbf{c}_q^\top \mathbf{c}_k + (\lambda_q \odot \mathbf{p}_s)^\top \mathbf{p}_k, \end{aligned} \quad (19)$$

where $\mathbf{c}_q, \mathbf{c}_k, \mathbf{p}_q, \mathbf{p}_k$ are the content query, content key, spatial query and spatial key, respectively. The content query consists of the embedding (\mathbf{p}_s) of the reference point, and the image-dependent transformation (λ_q).

For the first decoder layer, the cross attention weight of Conditional DETR [25] is calculated by:

$$(\mathbf{c}_q + \mathbf{o}_q)^\top (\mathbf{c}_k + \mathbf{p}_k) + \mathbf{o}_q^\top \mathbf{p}_k, \quad (20)$$

where \mathbf{o}_q is the object query. This is different from Eq. (19) since there is no image-dependent information as input in the first decoder layer of Conditional DETR [25].

By contrast, we adopt the same formulation for the first decoder layer as Eq. (19). The reference point is initialized from the image content and is likely to lie in the object regions. The sinusoidal embedding is applied to the reference point to obtain \mathbf{p}_s . The transformation (λ_q) that contains the scale information of the object is predicted from the corresponding encoder embedding of the reference point.

References

1. Beltagy, I., Peters, M.E., Cohan, A.: Longformer: The long-document transformer. CoRR **abs/2004.05150** (2020)
2. Bochkovskiy, A., Wang, C., Liao, H.M.: Yolov4: Optimal speed and accuracy of object detection. CoRR **abs/2004.10934** (2020)
3. Cai, Z., Vasconcelos, N.: Cascade R-CNN: delving into high quality object detection. In: CVPR (2018)
4. Carion, N., Massa, F., Synnaeve, G., Usunier, N., Kirillov, A., Zagoruyko, S.: End-to-end object detection with transformers. In: ECCV (2020)
5. Chen, X., Ding, M., Wang, X., Xin, Y., Mo, S., Wang, Y., Han, S., Luo, P., Zeng, G., Wang, J.: Context autoencoder for self-supervised representation learning. arXiv preprint arXiv:2202.03026 (2022)
6. Chen, X., Lin, K.Y., Qian, C., Zeng, G., Li, H.: 3d sketch-aware semantic scene completion via semi-supervised structure prior. In: CVPR. pp. 4193–4202 (2020)
7. Chen, X., Lin, K.Y., Wang, J., Wu, W., Qian, C., Li, H., Zeng, G.: Bi-directional cross-modality feature propagation with separation-and-aggregation gate for rgb-d semantic segmentation. In: ECCV. pp. 561–577. Springer (2020)
8. Chen, X., Yuan, Y., Zeng, G., Wang, J.: Semi-supervised semantic segmentation with cross pseudo supervision. In: CVPR. pp. 2613–2622 (2021)
9. Child, R., Gray, S., Radford, A., Sutskever, I.: Generating long sequences with sparse transformers. CoRR **abs/1904.10509** (2019), <http://arxiv.org/abs/1904.10509>
10. Choromanski, K., Likhoshesterov, V., Dohan, D., Song, X., Gane, A., Sarlós, T., Hawkins, P., Davis, J., Mohiuddin, A., Kaiser, L., Belanger, D., Colwell, L., Weller, A.: Rethinking attention with performers. CoRR **abs/2009.14794** (2020), <https://arxiv.org/abs/2009.14794>
11. Dai, Z., Cai, B., Lin, Y., Chen, J.: UP-DETR: unsupervised pre-training for object detection with transformers. CoRR **abs/2011.09094** (2020), <https://arxiv.org/abs/2011.09094>
12. Dai, Z., Yang, Z., Yang, Y., Carbonell, J.G., Le, Q.V., Salakhutdinov, R.: Transformer-xl: Attentive language models beyond a fixed-length context. In: ACL (2019)
13. Gao, P., Zheng, M., Wang, X., Dai, J., Li, H.: Fast convergence of DETR with spatially modulated co-attention. CoRR **abs/2101.07448** (2021), <https://arxiv.org/abs/2101.07448>
14. Glorot, X., Bengio, Y.: Understanding the difficulty of training deep feedforward neural networks. In: AISTATS (2010)
15. He, K., Zhang, X., Ren, S., Sun, J.: Deep residual learning for image recognition. In: CVPR (2016)
16. Ho, J., Kalchbrenner, N., Weissenborn, D., Salimans, T.: Axial attention in multidimensional transformers. CoRR **abs/1912.12180** (2019), <http://arxiv.org/abs/1912.12180>

17. Huang, Z., Wang, X., Huang, L., Huang, C., Wei, Y., Liu, W.: Ccnet: Criss-cross attention for semantic segmentation. In: Proceedings of the IEEE/CVF International Conference on Computer Vision. pp. 603–612 (2019)
18. Kitaev, N., Kaiser, L., Levskaya, A.: Reformer: The efficient transformer. In: ICLR (2020), <https://openreview.net/forum?id=rkgNKkHtvB>
19. Law, H., Deng, J.: Cornernet: Detecting objects as paired keypoints. In: Proceedings of the European conference on computer vision (ECCV). pp. 734–750 (2018)
20. Lin, T., Goyal, P., Girshick, R.B., He, K., Dollár, P.: Focal loss for dense object detection. TPAMI (2020)
21. Lin, T., Maire, M., Belongie, S.J., Hays, J., Perona, P., Ramanan, D., Dollár, P., Zitnick, C.L.: Microsoft COCO: common objects in context. In: ECCV (2014)
22. Liu, W., Anguelov, D., Erhan, D., Szegedy, C., Reed, S.E., Fu, C., Berg, A.C.: SSD: single shot multibox detector. In: ECCV (2016)
23. Liu, Z., Lin, Y., Cao, Y., Hu, H., Wei, Y., Zhang, Z., Lin, S., Guo, B.: Swin transformer: Hierarchical vision transformer using shifted windows. arXiv preprint arXiv:2103.14030 (2021)
24. Loshchilov, I., Hutter, F.: Fixing weight decay regularization in adam. In: ICLR (2017)
25. Meng, D., Chen, X., Fan, Z., Zeng, G., Li, H., Yuan, Y., Sun, L., Wang, J.: Conditional detr for fast training convergence. In: ICCV. pp. 3651–3660 (2021)
26. Peng, H., Pappas, N., Yogatama, D., Schwartz, R., Smith, N.A., Kong, L.: Random feature attention. CoRR **abs/2103.02143** (2021), <https://arxiv.org/abs/2103.02143>
27. Ramachandran, P., Parmar, N., Vaswani, A., Bello, I., Levskaya, A., Shlens, J.: Stand-alone self-attention in vision models. arXiv preprint arXiv:1906.05909 (2019)
28. Redmon, J., Farhadi, A.: YOLO9000: better, faster, stronger. In: CVPR (2017)
29. Redmon, J., Farhadi, A.: Yolov3: An incremental improvement. CoRR **abs/1804.02767** (2018)
30. Ren, S., He, K., Girshick, R., Sun, J.: Faster r-cnn: Towards real-time object detection with region proposal networks. Advances in neural information processing systems **28**, 91–99 (2015)
31. Ren, S., He, K., Girshick, R.B., Sun, J.: Faster R-CNN: towards real-time object detection with region proposal networks. TPAMI (2017)
32. Rezatofghi, H., Tsoi, N., Gwak, J., Sadeghian, A., Reid, I.D., Savarese, S.: Generalized intersection over union: A metric and a loss for bounding box regression. In: CVPR (2019)
33. Roy, A., Saffar, M., Vaswani, A., Grangier, D.: Efficient content-based sparse attention with routing transformers. ACL (2021), <https://transacl.org/ojs/index.php/tacl/article/view/2405>
34. Sun, Z., Cao, S., Yang, Y., Kitani, K.: Rethinking transformer-based set prediction for object detection. CoRR **abs/2011.10881** (2020), <https://arxiv.org/abs/2011.10881>
35. Tang, J., Chen, X., Wang, J., Zeng, G.: Not all voxels are equal: Semantic scene completion from the point-voxel perspective. In: AAAI. vol. 36, pp. 2352–2360 (2022)
36. Tang, J., Chen, X., Wang, J., Zeng, G.: Point scene understanding via disentangled instance mesh reconstruction. In: ECCV (2022)
37. Tian, Z., Shen, C., Chen, H., He, T.: FCOS: fully convolutional one-stage object detection. In: ICCV (2019)

38. Vaswani, A., Ramachandran, P., Srinivas, A., Parmar, N., Hechtman, B., Shlens, J.: Scaling local self-attention for parameter efficient visual backbones. In: CVPR. pp. 12894–12904 (2021)
39. Vaswani, A., Shazeer, N., Parmar, N., Uszkoreit, J., Jones, L., Gomez, A.N., Kaiser, L., Polosukhin, I.: Attention is all you need. In: NeurIPS (2017)
40. Wang, S., Li, B.Z., Khabsa, M., Fang, H., Ma, H.: Linformer: Self-attention with linear complexity. CoRR **abs/2006.04768** (2020), <https://arxiv.org/abs/2006.04768>
41. Wang, T., Yuan, L., Chen, Y., Feng, J., Yan, S.: Pnp-detr: Towards efficient visual analysis with transformers. In: ICCV. pp. 4661–4670 (2021)
42. Wang, Y., Zhang, X., Yang, T., Sun, J.: Anchor detr: Query design for transformer-based detector. arXiv preprint arXiv:2109.07107 (2021)
43. Xiong, Y., Zeng, Z., Chakraborty, R., Tan, M., Fung, G., Li, Y., Singh, V.: Nyströmformer: A nyström-based algorithm for approximating self-attention. CoRR **abs/2102.03902** (2021), <https://arxiv.org/abs/2102.03902>
44. Yuan, Y., Fu, R., Huang, L., Lin, W., Zhang, C., Chen, X., Wang, J.: Hrformer: High-resolution transformer for dense prediction. arXiv preprint arXiv:2110.09408 (2021)
45. Zaheer, M., Guruganesh, G., Dubey, K.A., Ainslie, J., Alberti, C., Ontañón, S., Pham, P., Ravula, A., Wang, Q., Yang, L., Ahmed, A.: Big bird: Transformers for longer sequences. In: NeurIPS (2020), <https://proceedings.neurips.cc/paper/2020/hash/c8512d142a2d849725f31a9a7a361ab9-Abstract.html>
46. Zhou, X., Wang, D., Krähenbühl, P.: Objects as points. CoRR **abs/1904.07850** (2019), <http://arxiv.org/abs/1904.07850>
47. Zhou, X., Zhuo, J., Krahenbuhl, P.: Bottom-up object detection by grouping extreme and center points. In: Proceedings of the IEEE/CVF conference on computer vision and pattern recognition. pp. 850–859 (2019)
48. Zhu, X., Su, W., Lu, L., Li, B., Wang, X., Dai, J.: Deformable DETR: deformable transformers for end-to-end object detection. CoRR **abs/2010.04159** (2020), <https://arxiv.org/abs/2010.04159>